OPTOELECTRONİCS AND ADVANCED MATERİALS – RAPİD COMMUNİCATİONS Vol. 3, No. 6, June 2009, p. 604 - 607

Current transport in GaSb /GaInAsSb/GaAlAsSb heterojunction photodiodes

M. AHMETOGLU (AFRAILOV)
Department of Physics, Uludag University, 16059, Görukle, Bursa, Turkey

Current flow mechanisms have been studied for Liquid Phase Epitaxy (LPE) grown n-GaSb / n-GaInAsSb / p-GaAlAsSb heterostructures lattice-matched to GaSb substrates. An experimental investigation of current-voltage characteristics has been done in the temperature range from 80–300K, and have been determined the mechanism of the flow of dark current. The qualitative comparison of experimental results with theory shows that, in the high temperature region the diffusion mechanism of the current flow dominates in both, forward and reverse biases. The tunneling charge has the key role at low temperatures under both forward and reverse biases.

(Received April 29, 2009; accepted June 15, 2009)

Keyword: Current flow mechanisms, Type II staggered-lineup, Broken-gap heterojunctions

1. Introduction

GaInAsSb / GaSb / GaAlAsSb hetero-structures have attracted a lot of scientific interest in the last few years mainly because of their importance for promising optoelectronic devices working in the wavelength region 1.5-4.8 μm. Both efficient light-emitting devices [1-3] and high-speed detectors [4-5] have been prepared and may be used for gas pollution monitoring, as well as for optical communica-tions in the new generation of fibers. The unusual band energy diagram in type II heterojunctions results in electron and holes being localized in self-consistent quantum wells on either side of the interface [6, 7]. Variation of the composition of $Ga_{1-x}In_xAs_{1-y}Sb_y$ can alter the degree of overlap of the energy bands at the heterojunction with GaSb so that both staggered-lineup and broken-gap hetero-junctions can be obtained [6]. In our previous work, we have reported the dark current mechanisms in isotype N^+ - n^0 - N^+ hetero-junctions [8]. GaSb-based materials are widely used narrow band gap semiconductors for infrared detection in 0.9-2.55 μm spectral range.

At the same time Thermophotovoltaic (TPV) devices based on III-V semiconductor alloys with bandgap energies corresponding to the mid-infrared wavelength range 2.2 to 2.5 μm (0.5 to 0.56 eV) are being developed. To date, the highest performing TPV devices in this wavelength range have been achieved for devices based on GaInAsSb and AlGaAsSb alloys lattice matched to GaSb substrates. The first 0.55-eV TPV cells in this materials system were reported at the Third NREL Conference on Thermophotovoltaic Generation of Electricity in 1997. Smaller-bandgap TPV devices have subsequently been reported with concurrent improvements in TPV device performance. This has largely been due to ongoing efforts to understand fundamental processes in materials growth, intrinsic materials properties, and their relationships to TPV device structure design and performance.

We presented results of investigations of current-voltage characteristics of photodiode structures on the base of Ga_{1-x} In_x As_y Sb_{1-y} with $x \leq 0.24$ which are known as the type II staggered-lineup heterojunctions. The results obtained will be useful both for improving the material synthesis technology and for developing optoelectronic devices.

2. Experimental

The structures were fabricated by liquid phase epitaxy method on n-type GaSb (III)B substrata, doped with Te to a carrier concentration of $(6\text{-}8)\times10^{17}$ cm^{-3}. The structures were actually double heterostructures, in which a narrow-gap n-GaInAsSb active layer (E_g = 0.54 eV at 300 K) was sandwiched between a GaSb substrate and a wide-gap p-GaAlAsSb layer. The wide-gap p-GaAlAsSb layer (optical window) with an aluminum content of about 34% forms a staggered junction to the narrow-gap layer. At the temperature of the epitaxial growth of the solid solution layer, it was isoperiodical with the GaSb substrate. Mesa samples with a working area 250-300 μm in diameter were fabricated from these structures by photolithography. The current-voltage (*I-V*) measurements were performed by the use of Keithley 2400 voltage source and capacitance-voltage measurements were per-formed by the use of KEITHLEY 590/1M *C-V* Analyzer using a temperature-controlled Janis CCS-150 cryostat, which enables us to make measurements in the temperature range of 10 - 360 K. All measurements were controlled by a computer via an IEEE-488 standard interface so that the data collecting, processing and plotting could be accomplished automatically.

3. Results and discussion

Have been studied the capacitance-voltage characteristics and the forward and reverse of the voltage-current characteristics. Fig. 1 shows the capacitance-voltage (*C-V*) characteristics taken at room temperature and frequency f =1 MHz.

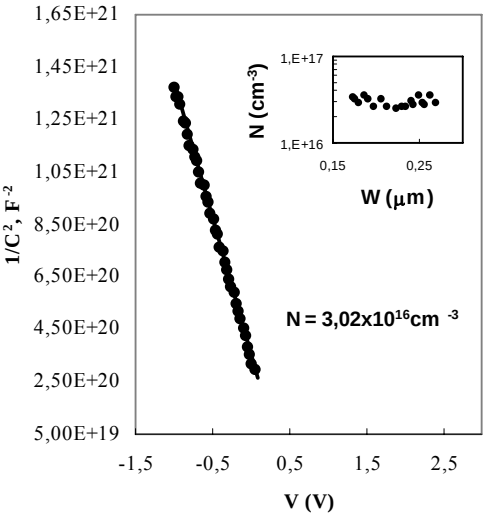

Fig. 1. Capacitance-voltage characteristics of the investigated of GaSb-GaInAsSb-GaAlAsSb heterojunctons at room temperature.

It is seen that, the p-n junctions obtained were an asymmetric abrupt, with $1/C^2 \sim f(V)$, and they had a wide space-charge (depletion) region, which lay mostly in the narrow-gap active region. The contact potential difference V_D found the linear dependence of C^{-2} on V (0.31 eV) coincides with the band offsets at the GaSb-GaInAsSb interface, in agreement with the data of [9,10]. Using the approximation of an asymmetric p-n junction of area S, we determined the donor concentration in the GaInAsSb narrow-gap layer:

$$C = S\sqrt{\frac{q\varepsilon_S N}{2(V_D - V)}} \qquad (1)$$

where ε_S is the dielectric constant. The values obtained lie in the range (2-4)x10^{16} cm^{-3}.

The non-uniformity of doping in the interface should manifest itself when considering the impurity density distribution, $N(x)$ is directly proportional to the first derivative of $1/C^2$ with respect to V and is given by [11],

$$N(x) = \frac{2}{q\varepsilon_S}\left[\frac{-d\left(1/C^2\right)}{dV}\right]^{-1} \qquad (2)$$

The above equation and relation $C = \frac{\varepsilon_S S}{W}$ are used to compute the doping profile of Fig.1 (the majority carrier densities versus depth (W) across the depleted zone). It is seen that the impurity density distribution is uniform with average doping concentration of N_d = 3.02 x10^{16} cm^{-3} (See inset of Fig. 1). No information is obtained at the interface ($x = 0$) as is typical for doping profiles obtained from $C-V$ measurements. This is because the capacitance measurement is limited to small forward bias current and the diffusion capacitance measurement.

The junction current as a function of applied bias, can be written in the following empirical form:

$$I = I_0\left[\exp\left(\frac{qV_a}{\beta kT}\right) - 1\right] \qquad (3)$$

where β is the ideality factor.

The comparison of theoretically calculated and experimental *I-V* characteristics in the forward bias region for several high temperatures are shown in Fig. 2.

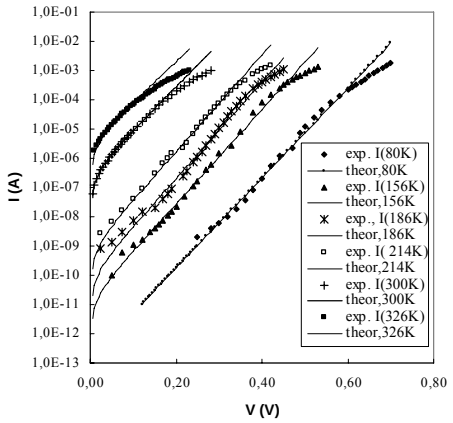

Fig. 2. Comparison of theoretically calculated (continuous line) and experimental (discrete points) I-V characteristics in the forward bias region at several temperatures.

It is seen that the β factor determined from the slope of the (I_F-V_F) characteristics at high temperatures ($T \geq 300$K) for small forward bias region, is equal to β = 1.1 ± 0.03 and indicates the predominantly diffusion nature of the current at investigated temperature range. The discrepancy from the theory for large forward bias voltages can be explained as due to the effect of series resistance.

The flow of holes from the p- region reaches the negative contact unimpeded, but electrons encounter a high barrier at the hetero-interface and find themselves in a deep potential well. Some electrons and holes with high energy pass over the barriers at the heterointerface.

However, the carrier recombination at the homojunction and at the heterointerface, with subsequent tunneling of carriers through it, makes a substantial contribution to the total current. At low temperatures, the tunneling processes become dominant, since passing over barriers becomes improbable. This is confirmed by the β values obtained ($\beta \geq 2$) for low temperature region.

Fig. 3 shows the reverse *I-V* charac-teristics at several temperatures. It is seen that, at room temperature, a quadratic dependence of the current on the bias is observed for small biases ($V \leq$ 0.4V, inset of Fig. 3), that indicating the predominance of the generative character of the current.

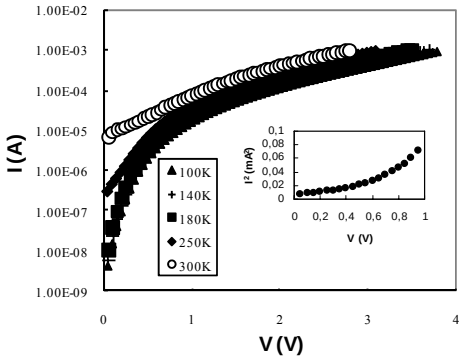

Fig. 3. Reverse current-voltage characteristics of GaSb-GaInAsSb-GaAlAsSb heterojunctions at several temperatures.

The generation and subsequent separation of carriers occur in the space-charge region of the $p-n$ junction in the narrow-gap layer. The effective carrier lifetime τ_{eff} was determined from this portion of the $I-V$ characteristic, using the known relation for the generation-recombination current [12]:

$$I = \frac{en_i WA}{\tau_{eff.}} \qquad (4)$$

where A is the junction area, W is the width of the space-charge region (proportional to $V^{1/2}$), n_i is the intrinsic carrier concentration at a given temperature.

The effective lifetime of carriers was calculated as $\tau_{eff..}$ = (6-9)×10^{-8} s from the dark current values obtained experimentally. The effective carrier lifetime is a key factor in the detectivity of a photodetector operating at about room temperature in the photovoltaic mode.

Fig. 4 shows the reverse current versus $10^3/T$ as a function of reverse bias. The activation energy, determining by this dependence at 0.1 V and the temperatures over the range from 300 K to 350 K was E_a = 0.28 ± 0.02 eV, this value was very nearly to a half band gaps value of narrow-gap structure. Estimations show that at high temperature region with reverse biases over 400 mV, the tunneling mechanism of the current dominates. This is confirmed by the weak temperature dependence of the current under reverse biases V > 0.4 V. At low temperature region, the current determined by tunneling over whole reverse bias range.

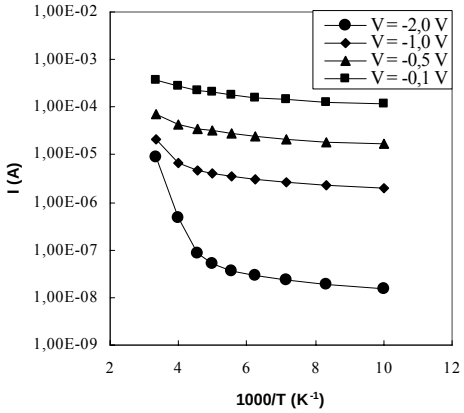

Fig. 4. The reverse current as a function of reciprocal temperature at different reverse applied bias.

To further test the tunneling model, the $I-V$ characteristics of the investigated samples were used to obtain the dependence of current on $1/E_m$ at fixed E_g, as shown in Fig. 5.

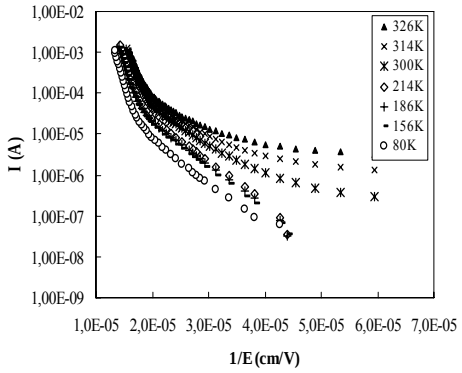

Fig. 5. Reverse biased dark current dependence on maximum electric field at several temperatures.

Note the tunneling current for direct gap semiconductors is strongly dependent on the ratio $E_g^{3/2}/E_m$, therefore, this mechanism can account for the nearly exponential dependence of dark current on applied voltage. The maximum junction electric field can be found experimentally by $E_m = \left[2qN_d\left(V_{bi} - V\right)/\varepsilon_2\right]^{1/2}$. The data show considerable curvature at low electric fields, with the curvature more pronounced at higher temperatures. This

behavior indicates that tunneling becomes the dominant source of leakage with increasing field and decreasing temperature.

4. Conclusions

We presented the results of dark current analysis of n-GaSb / n-GaInAsSb / p-GaAlAsSb type II staggered-lineup hetero-junctions studying in several temperatures. This work demonstrated diffusion current dominates at the high temperature in small forward bias region. The experimental results shows that the generation-recombination mechanism predomi-nant contribution of to reverse dark current at high temperatures and in small bias region. Estimations show that at high temperature region with reverse biases over 400 mV, the tunneling mechanism of the current dominates. Studies of these heterojunctions provided the physical basis for the fabrication of the photodetectors operating in the wavelength range 1.6 – 2.2 μm, important for third-generation infrared fiber-optic communication systems and suitable for tasks involving ecology and protection of the environment.

Acknowledgments

This work was supported by Uludag University, Scientific Research Project Unit grant No. 2007/36. The authors would like to thank the university for their support.

References

[1] L. M. Dolginov, L. M. Druzhinina, P. G. Eliseev, I. V. Kryukova, V. I. Leskovich, IEEE J. Quantum Electron. **QE-13**, 609 (1977).
[2] H. Kano, S. Miazava, K. Sugiyama, Electron. Lett. **16**, 146 (1980).
[3] A. N. Baranov, D. E. Dzhurtanov, A. N. Imenkov, A. A. Rogachev, Yu. M. Shernyakov, Yu. P. Yakovkev, Sov. Phys. Semicond. **20**, 1385 (1986).
[4] G. Bougnot, F. De Lannoy, J. Electro-chem. Soc. **135**, 783 (1988).
[5] A. N. Baranov, A. N. Imenkov, M. P. Mikhailova, A. A. Rogachev, Yu. P. Yakov-lev, Proc. SPIE **1048**, 188 (1989).
[6] M. P. Mikhailova, A. N. Titkov, Semicond. Sci. Technol. **9**, 1279 (1994).
[7] M. A. Afrailov, Infrared Phys. and Technol. **45**, 169 (2004).
[8] M. Ahmetoglu (Afrailov), I. A. Andreev, E. V. Kunitsyna, M. P. Mikhailova, Yu. P. Yakovlev, Semiconductors, **41**(2), 150 (2007).
[9] M. A. Afrailov, M. P. Mikhailova, N. R. Rahimov , Tr. J. of Phys. **21**, 1229 (1997).
[10] M. S. Bresler, O. B. Gusev, A. N. Titkov,et al., Semiconductors **27**, 341 (1993).
[11] H. Kroemer, Appl. Phys. Lett. **46**, 504, (1985).
[12] S. Sze, Physics of Semiconductor Devices, Wiley, New York, 1981.

*Corresponding author: afrailov@uludag.edu.tr